Published in final edited form as:
J Magn Reson Imaging. 2012 April ; 35(4): 891–898. doi:10.1002/jmri.22867.

Quantitative cartilage degeneration associated with spontaneous osteoarthritis in a guinea pig model

Matthew C. Fenty, BS[1], **George R. Dodge, PhD**[2], **Victor Babu Kassey, PhD**[1], **Walter R.T. Witschey, PhD**[1], **Arijitt Borthakur, PhD**[1], and **Ravinder Reddy, PhD**[1]

[1]CMROI, Department of Radiology, University of Pennsylvania School of Medicine, Philadelphia, PA

[2]McKay Orthopaedics Labs, Department of Orthopaedic Surgery, University of Pennsylvania School of Medicine, Philadelphia, PA

Abstract

PURPOSE—To determine (i) the feasibility and intra- and inter- scan reproducibility of $T_{1\rho}$ magnetic resonance imaging (MRI) in assessing cartilage degeneration in a guinea pig model with naturally occurring joint disease that closely mimics human osteoarthritis (OA), (ii) demonstrate the sensitivity of $T_{1\rho}$ MRI in assessing the age dependent cartilage degeneration in OA progression as compared to histopathological changes.

MATERIALS AND METHODS—Duncan-Hartley guinea pigs were obtained at various ages and maintained under an IACUC approved protocol. The left hind stifle joint was imaged using $T_{1\rho}$ MRI on a 9.4 Tesla Varian horizontal 20 cm bore scanner using a custom surface coil. Reproducibility of $T_{1\rho}$ MRI was assessed using four-month old guinea pigs (N=3). Three age cohorts; 3 month (N=8), 5 month (N=6), and 9 month (N=5), were used to determine the age-dependent osteoarthritic changes as measured by $T_{1\rho}$ MRI. Validation of age-dependent cartilage degeneration was confirmed by histology and Safranin-O staining.

RESULTS—$T_{1\rho}$ values obtained in the cartilage of the stifle joint in guinea pigs were highly reproducible with an inter-scan mean coefficient of variation (CV) of 6.57% and a maximum intra-scan CV of 9.29%. Mean cartilage $T_{1\rho}$ values in animals with late stage cartilage degeneration were 56.3 – 56.9 ms (5 – 9 month cohorts) were both significantly ($p<0.01$) higher than that obtained from 3-month old cohort (44 ms) demonstrating an age-dependent variation. $T_{1\rho}$ was shown to be significantly greater than T_2. $T_{1\rho}$ dispersion was observed in this animal model for the first time showing an increase of 45% between 500Hz and 1500Hz spin-locking frequency. Cartilage thickness measurements were calculated from single mid-coronal histology sections from same animals used for $T_{1\rho}$ MRI. Thickness calculations showed insignificant differences between 3- and 5 month cohorts and was significantly decreased by 9-months of age ($p<0.01$). A moderate correlation ($R^2=0.45$) existed between $T_{1\rho}$ values and signal intensity of Safranin-O stain.

CONCLUSION—The data presented demonstrate that $T_{1\rho}$ MRI is highly reproducible in this spontaneous model of OA and may serve as a noninvasive tool to characterize joint cartilage degeneration during OA. Age-dependent changes, verified with histological measurements of proteoglycan loss, correlated with $T_{1\rho}$ across different age groups. $T_{1\rho}$ has adequate dynamic

Address for Correspondence: Matthew Fenty, CMROI, Department of Radiology, University of Pennsylvania, B1 Stellar-Chance Laboratories, 422 Curie Boulevard, Philadelphia, PA 19104-6100, Tel: (215) 898-9357, Fax: (215) 573-2113, MFenty@UPenn.edu, Web: http://cmroi.med.upenn.edu/.

CONFLICT OF INTEREST

The authors have no conflict of interest regarding the subject matter discussed.

range and is sensitive to detect and track the progression of cartilage degeneration in the guinea pig model before gross anatomical changes such as cartilage thinning has occurred. This study presents a technological advancement that would permit longitudinal studies of evaluating disease-modifying therapies useful for treating human OA.

Keywords

osteoarthritis; $T_{1\rho}$ MRI; animal model; quantitative

INTRODUCTION

Osteoarthritis (OA) is a common and painful condition with a multi-factorial etiology of the musculoskeletal system affecting more than 50% of the U.S. population over 65 (1,2). Early progression of the disease is usually subtle with clinical manifestation occurring in the later stages of the disease. Degeneration of the articular cartilage tissue, which many believe to be a primary factor in the development of OA, is a slow process and typically takes decades to have full thickness loss, but can be significantly accelerated due to trauma or surgical procedures (3). Subsequently, permanent and irreversible damage of the joint has often occurred by the time a clinical diagnosis is made, either by non-invasive joint space measurements via radiography or invasive arthroscopy to examine the joint tissue. Currently there is no cure for the disease and therapeutic interventions are primarily targeted to symptomatic relief. Therefore, it is highly desirable to develop an accurate and sensitive method for early diagnosis and monitoring of OA in patients. Moreover, a non-invasive technique that is sensitive to a relevant tissue biomarker related to early degenerative changes in cartilage would be preferable for longitudinally monitoring OA progression and testing novel treatment methods.

Animal models of OA serve as a bridge between *ex vivo* tissue analysis and *in vivo* studies. Apart from surgical or artificially induced cartilage degeneration, several animal models such as mice, guinea pigs, macaques, and beagles have been shown to spontaneously develop OA (4). Among these animals, Dunkin-Hartley guinea pigs have been shown to develop OA with the earliest stage of detection manifesting as early as three to four months of age. Therefore, the Dunkin-Hartley guinea pig model provides a more practical system for the longitudinal studies of the progression of OA (3, 5, 6).

While MRI has been used to detect compositional and morphological changes in the cartilage of the Dunkin-Hartley guinea pigs using T_1 and T_2 contrast (7), current protocols are not sensitive to the early stages of OA marked by proteoglycan (PG) loss from the extracellular matrix (ECM) of articular cartilage (8, 9, 10). Newer methods, such as delayed gadolinium enhanced MRI of cartilage (dGEMRIC), are promising, but logistic issues such as long waiting periods following the contrast injection, and the need for pre-injection T_1 maps, reduce its utility. On the other hand, sodium MRI is a highly specific biomarker for PG, inherently suffers from both low signal and resolution and also requires special hardware (11,12). In this context, $T_{1\rho}$ MRI, a proton-based method that has the ability to generate endogenous contrast *in vivo* based on cartilage molecular content (13), is a more desirable alternative.

$T_{1\rho}$ is the spin-lattice relaxation time in the rotating frame and is sensitive to the slow-motion interactions (~few Hz to several kHz) such as exchange of hydroxyl and amide group protons on glycosaminoglycan chains of PG with bulk water protons (14) and has been shown to correlate with cartilage proteoglycan content (11, 14). $T_{1\rho}$ has been shown to increase linearly with PG loss in controlled degradation experiments performed on *ex vivo* bovine patellae samples (14, 15), in the porcine model of IL-1β induced cartilage

degeneration (16), and in humans with chondromalacia (17). However, there have been no $T_{1\rho}$ MRI studies in the Dunkin-Hartley guinea pig model with naturally occurring joint disease that closely mimics human OA. In this study, we determine the reproducibility of $T_{1\rho}$ MRI *in vivo* and use it to track the well-known age-dependent cartilage degeneration verified subsequently by histopathology measurements.

MATERIALS AND METHODS

Animal protocol

The study was approved by the Institutional Animal Care and Use Committee (IACUC). Female Dunkin-Hartley guinea pigs (Charles River Labs, Malvern, PA; Elm Hill Laboratory, Chelmsford, MA) were used in the study and all assessments were made on the left hind stifle. Three separate age cohorts were utilized for age dependent variation assessments: three-month old (N=8), five month old (N=6), and nine month old (N=5). Four month old animals (N=3) were used for reproducibility measurements.

Immediately before imaging, each animal was anesthetized in an induction chamber using 4% isoflurane/O_2 mixture at a flow rate of 2.5 L/min for 10 minutes. Animals were then transferred to a custom-made housing platform and placed in the prone position where the hind leg was secured. A custom-made nose cone was placed on the animal's head delivering anesthesia. The stifle was secured so that load bearing femoral condyle was normal to the tibial plateau which required the joint to be flexed to ~115°. A custom built MRI curved rectangular transceive surface coil (4 cm × 2 cm) was positioned and secured anterior to the joint. After the animal was placed inside the bore, anesthesia was lowered to 1.5–2.5% isoflurane/O_2 mixture at 1.5 L/min flow rate for the duration of the imaging session. Body temperature was continuously monitored with a rectal probe and maintained at 37–40°C through a feedback–controlled heater. Heart rate was monitored using subdural electrocardiogram (ECG) leads.

$T_{1\rho}$ MRI

$T_{1\rho}$ MRI pulse sequence based a $T_{1\rho}$-prepared 3D balanced gradient echo (b-GRE) for a fast volumetric acquisition (18) was coded on a Varian (Varian Inc. Palo alto, CA) pulse-programming environment (Figure 1). The $T_{1\rho}$-prepared signal decays exponentially as a function of spin-lock pulse duration (TSL) and multiple images generated with varying TSL times are acquired in each imaging session. These $T_{1\rho}$-weighted images are then fitted pixel-wise to the known signal decay function to generate color-coded $T_{1\rho}$ parametric maps.

Reproducibility measurements

Four-month old animals (N=3) were scanned repeatedly during three separate MRI sessions over the course of two days. $T_{1\rho}$ maps were calculated and values were averaged from four compartments (medial/lateral femoral/tibial) of cartilage. Coefficients of variation (standard deviation/mean, CV) were calculated to determine inter- and intra-animal reproducibility.

MRI protocol

MRI was performed on a 9.4 Tesla horizontal 20cm bore animal scanner (Varian Inc., Palo Alto, CA). B_0 calibration was performed first through scanner default calibration then through localized voxel shimming. A spectral line-width less than 50 Hz was maintained through the center of the joint space. B_1 calibration was performed using a "flip-crush" procedure in which a single hard-pulse of arbitrary amplitude and fixed duration followed by gradient crushers with a generic gradient-echo imaging readout immediately following. A series of rapid image acquisition was performed while titrating the hard-pulse amplitude

until a signal minimum (flip=90°) was achieved along a band within the center of the joint. These calibrations were used for all subsequent imaging.

3D b-GRE $T_{1\rho}$ MRI sequence was then used with the following parameters: FOV = 30 mm × 30 mm, slab thickness = 8 mm, acquisition matrix = 512 × 256 × 16 – interpolated to 512 × 512 × 16, resolution = 59 μm × 59 μm × 500 μm, α = 20°, centric encoding, TE = 5ms, TR = 9ms. A four-shot segmented acquisition was used to mitigate loss of $T_{1\rho}$-contrast while residual signal approached the steady state. A delay of 3.5 seconds was appended to the end of each segment to allow full recovery of the longitudinal magnetization between $T_{1\rho}$-preparatory segments. The spin-lock amplitude was fixed at 1500Hz for all $T_{1\rho}$-weighted acquisitions and the spin-lock durations were varied (TSL = 1, 10, 20, 30, 40 ms) for subsequent $T_{1\rho}$ mapping.

Raw k-space data were filtered to reduce blurring due to transient signal decay as described previously (18). Total imaging time was ~20 minutes per TSL using four signal averages. High-resolution T_1-weighted images were acquired using the b-GRE sequences to allow for cartilage segmentation. Human $T_{1\rho}$ MRI studies routinely utilize a heavily T_1-weighted or MPRAGE image set to easily distinguish bone and meniscus from cartilage within the joint. The T_1-weighted imaging parameters were $T_{1\rho}$ parameters excluding the $T_{1\rho}$-preparation pulse. The acquisition was a linear and non-segmented with signal averages increased to 8.

$T_{1\rho}$ mapping

Images were transferred via FTP and processed on a Dell Dimension computer (Dell Inc, Round Rock, TX). All $T_{1\rho}$-weigted images for each animal were automatically co-registered to the shortest TSL image data set using a 2D rigid body co-registration algorithm written in C for MATLAB (The Math Works, Natick MA). After co-registration was complete, the acquired $T_{1\rho}$-weighted images were fit to the linearized mono-exponentially decaying $T_{1\rho}$ function using linear least square algorithm and a correlation coefficient (R^2) of the fit was calculated. The $T_{1\rho}$ relaxation maps contain only those fit with $R^2 > 0.90$.

The stifle joint cartilage was manually segmented by a single user (M.F.) from the T_1-weighted images by using SliceOMatic software (Tomovision, Quebec, CA). Mid-coronal slices of the stifle were used to segment cartilage into four compartments i.e. medial/lateral tibial/femoral. Segmented masks were then used to automatically record mean $T_{1\rho}$ values in each compartment to an Excel spreadsheet (Microsoft, Inc., Redmond, WA). Of the 16 $T_{1\rho}$-weighted slices acquired for each animal, $T_{1\rho}$ values were obtained from the center load-bearing portion of the stifle which utilized 4–6 slices. For the purpose of this study, compartment values for each slice were averaged to determine an individual global compartment $T_{1\rho}$ value.

$T_{1\rho}$ Dispersion Mapping

One 3-month old animal was scanned to determine $T_{1\rho}$ dispersion i.e. $T_{1\rho}$ values in cartilage as a function of spin-lock frequency ($\gamma B_1/2\pi$). Four separate $T_{1\rho}$ maps were generated with varying (500, 1000, 1500, 2000Hz) spin-lock amplitudes. $T_{1\rho}$ imaging parameters and processing techniques were as described above. T_2 maps were acquired with single mid-coronal slice TSE/FSE pulse sequence with the following imaging parameters: TR = 3.5 s, TE = 10, 20, 40, 80 ms, Train Length = 8, FOV = 30 mm × 30 mm, Slice Thickness = 1 mm, Acquisition Matrix = 256 × 256. T_2 was calculated and recorded in a similar manner to $T_{1\rho}$ as explained above and used for the data point at a spin-lock frequency of 0Hz.

Histochemical Analysis

Cartilage tissue was examined histologically to visualize and quantify PG content. Immediately after imaging, each animal was euthanized by a certified veterinary technician via intra-cardiac injection of highly concentrated medical-grade KCl solution as approved by the IACUC. The animals were stored frozen (−20° C) and collectively processed. The imaged hind limb (left) was dissected clean of soft tissue and the joint exposed. Each joint was fixed in 10% buffered formalin (Fisher) for 15 days followed by decalcification using Formical-2000 (Decal Chemical, Tallman, NY) until chemical testing for calcium was negative. The bones were then processed for routine paraffin embedding and histology with coronal sections 8μm thick. Sections were de-paraffinized and stained with Safranin-O by routine procedures (19). A quantitative analysis was performed of calculating staining intensity using ImageJ (NIH, Bethesda MD). Single mid-coronal weight-bearing sections for each animal were determined as a representative slice for the entire joint. Four ROIs, defined above, were utilized for each animal and the relative staining intensity of a single color channel was determined.

Cartilage Thickness

Histological sections were used to measure cartilage thickness as they are the most precise with highest pixel resolution. Each compartment for each animal was measured at its thickest point normal to the load-bearing portion of the joint. For the femur, this was in the center of each condyle and for the tibia, it was in the center of each side of the plateau. A single line extending from the superficial surface to the calcified-noncalficied cartilage tidemark was drawn.

Cartilage thickness was additionally measured with a signal mid-coronal load-bearing T_1-weighted image. To minimize errors between measurements, a single thickness measurement was calculated in the center of the lateral tibial plateau.

RESULTS

The entire protocol was able to acquire 3D data sets for $T_{1\rho}$ mapping in less than two hours. Optimization of the MRI pulse sequences and protocol resulted in high resolution high contrast images in very thin cartilage (~200μm) of guinea pigs (Figure 2A). Typical T_1-weighted images show remarkably high contrast between cartilage and surrounding tissue in the stifle joint (Figure 2B), facilitating cartilage segmentation (Figure 2C) for automated reporting of $T_{1\rho}$ values from the parametric maps that were calculated from images with varying $T_{1\rho}$-weighting (Figure 3). The reproducibility of $T_{1\rho}$ measurements is summarized in Table 1. Maximum CV was <10% indicating a high precision in mapping and quantifying $T_{1\rho}$ in guinea pig cartilage *in vivo* using this protocol. $T_{1\rho}$ dispersion in guinea pig cartilage (Figure 4) was observed for the first time. An average T_2 of 3-month old cohort's cartilage was calculated (11.75 ms) and used as the value for spin-lock frequency of 0 Hz. $T_{1\rho}$ increased by 45% between 500Hz and 1500Hz (31.7ms to 42.5 ms).

Representative $T_{1\rho}$ maps from each cohort, combined $T_{1\rho}$ distribution histograms for all animals, and representative histological sections from each age cohort are shown (Figure 5). $T_{1\rho}$ maps are shown superimposed on their corresponding T_1-weighted image (Figure 5, 1st row). Quantitative analysis show increased $T_{1\rho}$ values and qualitative analysis demonstrates increased visual heterogeneity in older cohorts compared to the 3-month animal. $T_{1\rho}$ distribution histograms (Figure 5, 2nd row) show a strong but non-significant positive skew in increasing age. Histological assessments confirm progression of spontaneous OA with age (Figure 5, 3nd row) as seen by decreased stain intensity and cartilage thinning.

Cartilage thickness measurements were measured from a single mid-coronal histological section for each animal and mean values are shown (Figure 6, Figure 7). The average thickness of cartilage was insignificantly different between the 3- and 5-month old cohorts. There are significant differences in thickness between the 3- and 5-month old cohorts as compared to the 9-month cohort indicating that gross anatomic changes to thickness occur later than elevated $T_{1\rho}$ or PG loss. Cartilage thickness was also calculated from high-resolution MR images for each joint. We observe similar differences in thickness between the 3- and 5- month old cohorts with the more degenerated 9- month old cohort (Figure 8). Normalized Safranin-O stain intensity versus $T_{1\rho}$ value was plotted for all animals (Figure). Each animal's stain intensity and $T_{1\rho}$ values were averaged for all compartments to generate a single value for each metric. The plot depicts an inverse relationship with decreasing PG implying higher $T_{1\rho}$.

DISCUSSION

This study demonstrates the feasibility of *in vivo* quantification of cartilage degeneration in the guinea pig model by using $T_{1\rho}$ MRI. The resulting MRI protocol was well tolerated by the animals and the reproducible measurements suggest that this protocol may be suitable for studies tracking progression of cartilage degeneration longitudinally as well as to monitor the effects of therapeutic intervention non-destructively and potentially with fewer animals.

While histological measurements are regarded as the gold standard in quantifying OA severity, it requires post-mortem examination and cannot be used to monitor the progression of OA *in vivo.* Accurate quantification of proteoglycan levels requires staining be carried out simultaneously on all tissues to ensure relative staining intensities are preserved.

Both inter- and intra- animal COVs were noticeably small indicating a high precision of the $T_{1\rho}$ measurement protocol for use in this model of OA. Future studies will need to examine the reproducibility of this protocol on symptomatic cohorts to ensure changes in biochemical composition and thickness to not significantly alter recorded $T_{1\rho}$ measurements.

The $T_{1\rho}$ dispersion observed in the guinea pig cartilage is due to the mitigation of relaxation effects such as B_0 inhomogenieties, residual dipolar interaction, magic angle effects, and processes such as chemical exchange (13). For this reason, $T_{1\rho}$ relaxation time is always greater than T_2 and possesses a higher dynamic range. This leads to increased sensitivity of $T_{1\rho}$ to changes in cartilage macromolecules compared to T_2 (17,20). Due to difficulties in accurate B_0 shimming on this magnet, inherent low T_2 values of cartilage, and difficulties with adequate SNR, $T_{1\rho}$ MRI was preferred. $T_{1\rho}$ MRI is capable of additional B_0 corrections, larger dynamic range of $T_{1\rho}$ values, and increased SNR due to decreased relaxation effects.

$T_{1\rho}$ dispersion may provide to be a quantifiable metric that can be utilized to diagnose osteoarthritis severity. However, for the purpose of this work, $T_{1\rho}$ dispersion calculations were utilized to empirically determine a practical spin-lock amplitude. Utilizing a high-amplitude spin-lock, $T_{1\rho}$ MRI was able to mitigate the dominate dipolar interactions which are significant at high fields. Future studies addressing dispersion characteristics in this model may provide an additional tool for the diagnosis and quantification of this disease.

It should be noted that previously reported $T_{1\rho}$ values in clinical studies typically did not exceed a spin-lock frequency of 500 Hz. This is due to SAR limitations in order to keep RF energy deposition at a minimum and due to hardware limitations. In this study, we were able to utilize 1500 Hz frequency without causing any distress to the animals as determined by the careful monitoring of its vital signs and visual inspection of the joint pre- and post-

imaging. MRI relaxation interactions such as susceptibility and residual dipolar interaction can be mitigated by using the higher spin-lock frequency. At high field strength MRI scanners such as the 9.4T used in this study, intrinsic cartilage T_2 is expected to be ~10 ms and is significantly shorter than the corresponding values on 1.5T and 3T clinical scanners. The short T_2, due to a predominant residual dipolar interaction associated with the collagen component of cartilage, precludes the reliable detection of any early molecular changes due to poor signal characteristics.

Given the size of the guinea pig joint and specialized hardware available, it is feasible to use high spin lock frequencies that will significantly improve the dynamic range of $T_{1\rho}$ enabling the detection of very early molecular changes that occur during the OA process. Imaging with a 500 Hz spin-lock frequency at 9.4T will provide $T_{1\rho}$ values less than those calculated at 1500 Hz. With incomplete mitigation of high-field relaxation effects, the $T_{1\rho}$ signal will be less sensitive to changes in biochemical composition.

Significant $T_{1\rho}$ changes were observed between 3-month and 5-month old cohorts while the cartilage thickness remained unchanged potentially providing evidence that $T_{1\rho}$ may be more sensitive to the early macromolecular changes that occur with cartilage degeneration as compared to morphological changes in this animal model of OA. Thickness measurements from MR images show similar trends to those calculated from histology. Discrepancies between measurements are from resolution differences between two imaging methods (59 μm vs. 1.2 μm in-plane resolution). Partial voluming effects and non-consistent tissue thickness pose a significant limitation to accurately determine cartilage thickness *in vivo.* However, with these limitations, similar trends between histology and MR show significant thickness differences during late stage disease manifestation.

There are limitations when using a single histological section in determining cartilage thickness. Inherent variations in thickness among the surface will cause variations between measurements. However, while discrepancies may arise, larger differences are believed to be due to substantial losses in cartilage thickness. Further detailed analysis of cartilage thickness measurements will need to be addressed. These thickness measurements suggest that significant molecular changes occur within two months in this model from the baseline and these changes to the biochemical composition of joint cartilage can be quantified using $T_{1\rho}$ MRI.

Heterogeneous distribution of $T_{1\rho}$ values can be seen within the older cohorts suggests evidence of non-uniform cartilage degenerations. Visual inspection of histology sections show similar non-uniform staining throughout the joint surface and the layers of the cartilage. Regions of elevated mean $T_{1\rho}$ possibly include focal cartilage defects and non-uniform cartilage thinning. As with other clinical studies analyzing $T_{1\rho}$ in cartilage, regions of focal defects may be masked by compartmental averaging. One of the limitations of the study is the different thickness of MRI and histology slices (500μm vs. 8μm, respectively) used to analyze the data. Despite this limitation, correlation between $T_{1\rho}$ and histological stain intensities is rather reasonable. Additional correlations of $T_{1\rho}$ and immunohistochemistry will need to be assessed to further validate the biochemical changes to the articular cartilage of the joint.

Despite the inherent challenges associated with maintaining consistent staining throughout all sections and with smaller section slice thickness compared to MRI, a progressive reduction of stain intensity implying loss of PG is related to an increase in $T_{1\rho}$ as a function of age.

The endogenous nature of the $T_{1\rho}$ contrast provides a suitable quantitative biomarker for *in vivo* imaging of cartilage degeneration in the guinea pig model. Given the rapid

degeneration of cartilage with age in the guinea pig model, this study demonstrates the feasibility and practicality for $T_{1\rho}$ MRI in monitoring the progression of spontaneous cartilage degeneration within this guinea pig model. This noninvasive MRI approach with the sensitivity presented in this study provides may provide a useful platform for quantifying longitudinal changes in cartilage *in vivo* and may provide a practical model to assess the therapeutic benefit of new disease modifying therapies relevant to human OA as well provides insights into the early molecular changes that occur during the disease.

In conclusion, our study supports $T_{1\rho}$ as a relevant biomarker to detect changes in cartilage degeneration and track OA progression in animal models and could serve as a reliable surrogate to invasive methodology. While there is a reasonable correlation between $T_{1\rho}$ and the proteoglycan loss as measured from histological images, it is anticipated that additional analysis with more animals in expanded cohorts will improve the correlation. This platform is highly translatable to the pre-clinical environment and may be useful to both detect OA disease early and track the efficacy of potential disease modifying therapies.

Acknowledgments

Authors acknowledge technical support from the Small Animal Imaging Facility (SAIF) at the University of Pennsylvania's School of Medicine, in particular, the efforts of Dr. Steve Pickup.

This work was performed at the Center for Magnetic Resonance and Optical Imaging of NCRR (P41RR02305) and supported by the following NIH grants from NIAMS: R01AR051041, R01AR045404.

References

1. Felson D, Zhang Y, Hannan M, et al. The incidence and natural history of knee osteoarthritis in the elderly. The Framingham Osteoarthritis Study. Arthritis Rheum. 1995; 38(10):1500–1505. [PubMed: 7575700]
2. Seibel, MJ.; Robins, SP.; Bilezikian, JP. Dynamics of bone and cartilage metabolism. Vol. xx. San Diego: Academic Press; 1999. p. 672
3. Moskowitz, RW. Osteoarthritis : diagnosis and medical/surgical management. Vol. xx. Philadelphia: Saunders; 2001. p. 674676 p. of plates p
4. Pritzker K. Animal models for osteoarthritis: processes, problems and prospects. Ann Rheum Dis. 1994; 53(6):406–420. [PubMed: 8037500]
5. McDougall J, Andruski B, Schuelert N, Hallgrímsson B, Matyas J. Unravelling the relationship between age, nociception and joint destruction in naturally occurring osteoarthritis of Dunkin Hartley guinea pigs. Pain. 2009; 141(3):222–232. [PubMed: 19081191]
6. Tessier J, Bowyer J, Brownrigg N, et al. Characterisation of the guinea pig model of osteoarthritis by in vivo three-dimensional magnetic resonance imaging. Osteoarthritis Cartilage. 2003; 11(12): 845–853. [PubMed: 14629960]
7. Watson P, Carpenter T, Hall L, Tyler J. MR protocols for imaging the guinea pig knee. Magn Reson Imaging. 1997; 15(8):957–970. [PubMed: 9322215]
8. Grushko G, Schneiderman R, Maroudas A. Some biochemical and biophysical parameters for the study of the pathogenesis of osteoarthritis: a comparison between the processes of ageing and degeneration in human hip cartilage. Connect Tissue Res. 1989; 19(2–4):149–176. [PubMed: 2805680]
9. Lohmander L. Articular cartilage and osteoarthrosis. The role of molecular markers to monitor breakdown, repair and disease. J Anat. 1994; 184 (Pt 3):477–492. [PubMed: 7928637]
10. Goldring M. The role of the chondrocyte in osteoarthritis. Arthritis Rheum. 2000; 43(9):1916–1926. [PubMed: 11014341]
11. Wheaton A, Borthakur A, Shapiro E, et al. Proteoglycan loss in human knee cartilage: quantitation with sodium MR imaging--feasibility study. Radiology. 2004; 231(3):900–905. [PubMed: 15163825]

12. Shapiro E, Borthakur A, Dandora R, Kriss A, Leigh J, Reddy R. Sodium visibility and quantitation in intact bovine articular cartilage using high field (23)Na MRI and MRS. J Magn Reson. 2000; 142(1):24–31. [PubMed: 10617432]

13. Borthakur A, Mellon E, Niyogi S, Witschey W, Kneeland J, Reddy R. Sodium and T1rho MRI for molecular and diagnostic imaging of articular cartilage. NMR Biomed. 2006; 19(7):781–821. [PubMed: 17075961]

14. Palmer, Ar; Kroenke, C.; Loria, J. Nuclear magnetic resonance methods for quantifying microsecond-to-millisecond motions in biological macromolecules. Methods Enzymol. 2001; 339:204–238. [PubMed: 11462813]

15. Santyr G, Henkelman R, Bronskill M. Spin locking for magnetic resonance imaging with application to human breast. Magn Reson Med. 1989; 12(1):25–37. [PubMed: 2607958]

16. Wheaton A, Dodge G, Borthakur A, Kneeland J, Schumacher H, Reddy R. Detection of changes in articular cartilage proteoglycan by T(1rho) magnetic resonance imaging. J Orthop Res. 2005; 23(1):102–108. [PubMed: 15607881]

17. Witschey W, Borthakur A, Fenty M, et al. T1rho MRI quantification of arthroscopically confirmed cartilage degeneration. Magn Reson Med. 2010; 63(5):1376–1382. [PubMed: 20432308]

18. Witschey W, Borthakur A, Elliott M, et al. T1rho-prepared balanced gradient echo for rapid 3D T1rho MRI. J Magn Reson Imaging. 2008; 28(3):744–754. [PubMed: 18777535]

19. Schmitz N, Laverty S, Kraus V, Aigner T. Basic methods in histopathology of joint tissues. Osteoarthritis Cartilage. 2010; 18 (Suppl 3):S113–116. [PubMed: 20864017]

20. Li X, Han ET, Ma CB, Link TM, Newitt DC, Majumdar S. In vivo 3T spiral imaging based multi-slice T(1rho) mapping of knee cartilage in osteoarthritis. Magn Reson Med. 2005; 54(4):929–936. [PubMed: 16155867]

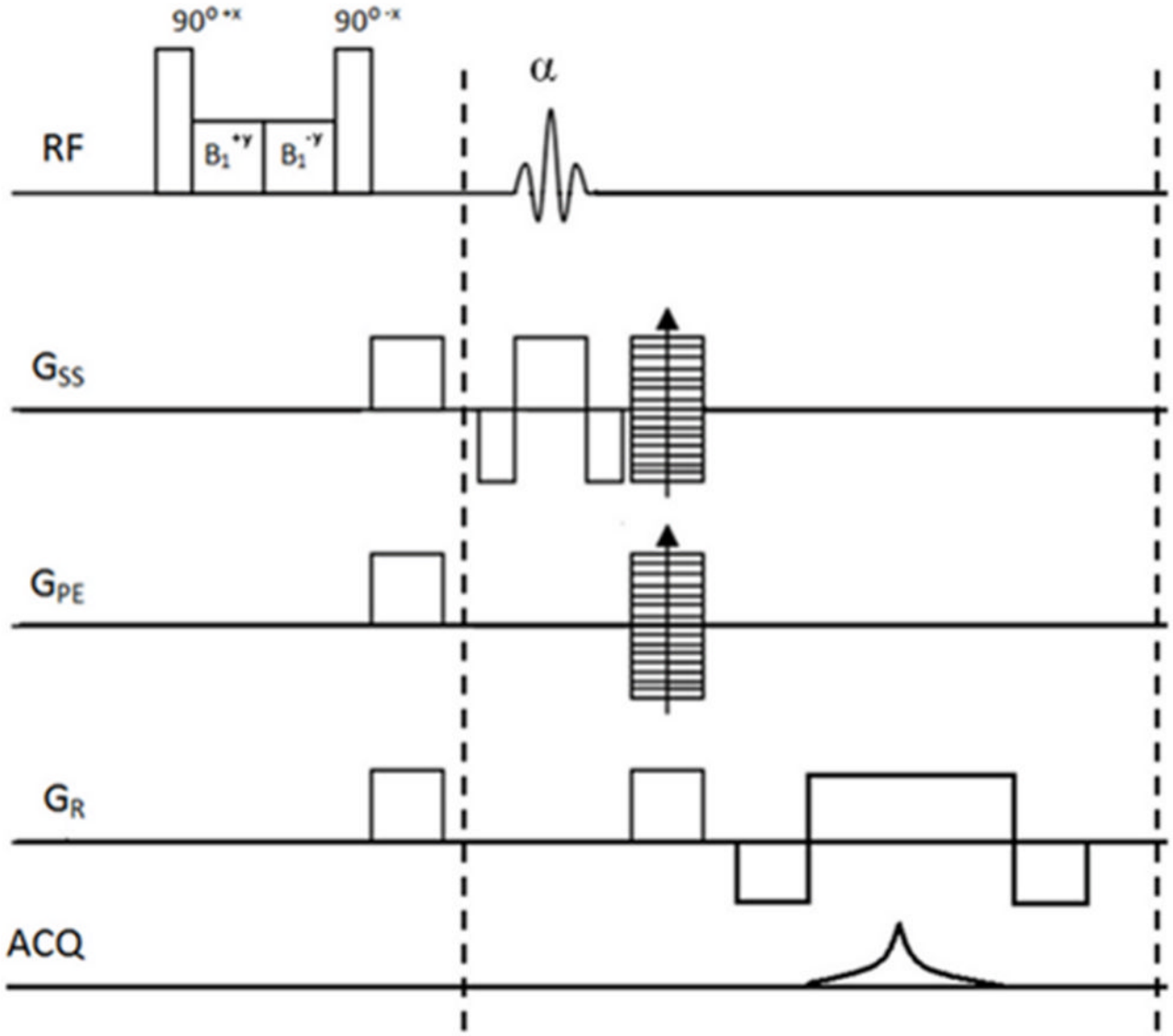

Figure 1.
The 3D balanced Gradient Echo (b-GRE) pulse sequence with appended $T_{1\rho}$ preparatory pulse cluster used for the studies. Sequence was implemented on a Varian MRI scanner and is able to obtain 16 slices in under 20 minutes of imaging time.

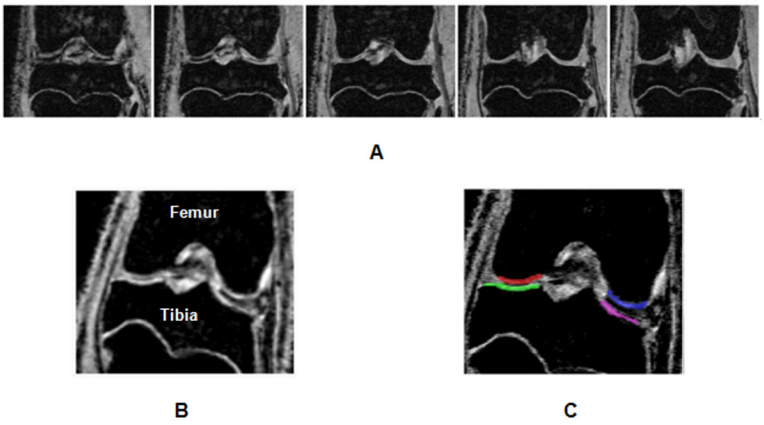

Figure 2.

The $T_{1\rho}$ MRI protocol implemented for this study provides images of the entire load-bearing portion of the stifle joint. Representative data of five slices from a data set of 16 slices as shown (A). The high contrast between cartilage and bone (B) facilitates easy segmentation of cartilage into four regions i.e. medial/lateral and femoral/tibia regions of interest (indicated by the color overlays in C).

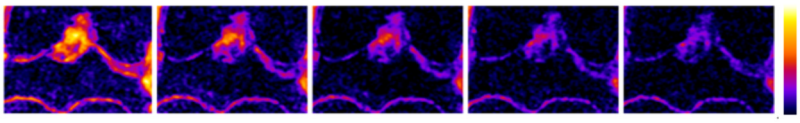

Figure 3.
Example of $T_{1\rho}$ contrast in the mid-coronal slice of the stifle joint is shown as color coded images (scale on the right). The apparent signal decay is a function of spin-lock pulse duration (TSL) equal to 1, 10, 20, 30, 40 ms from left to right, respectively.

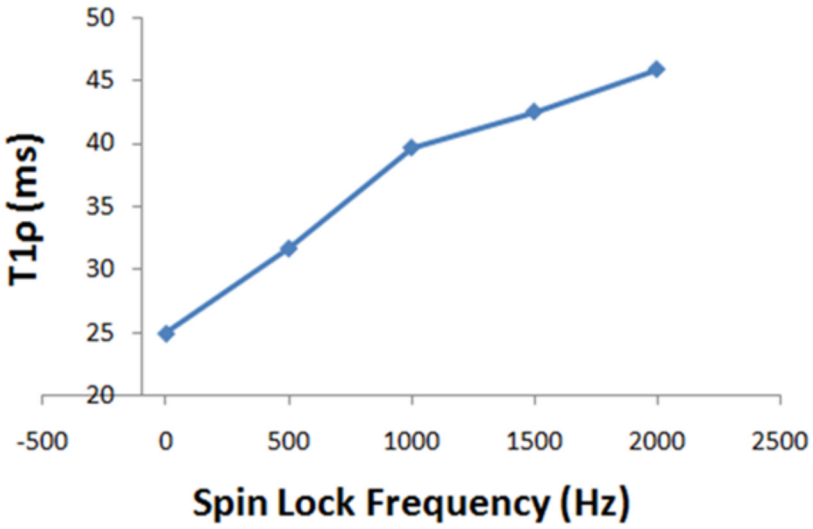

Figure 4.

$T_{1\rho}$ dispersion was observed in guinea pig cartilage demonstrating greater values for $T_{1\rho}$ even at 500Hz spin-locking frequency ($\gamma B_1/2\pi$) compared to T_2 (~spin-locking at 0Hz frequency). This implies greater sensitivity of $T_{1\rho}$ compared to T_2 in detecting macromolecular changes in tissues such as cartilage.

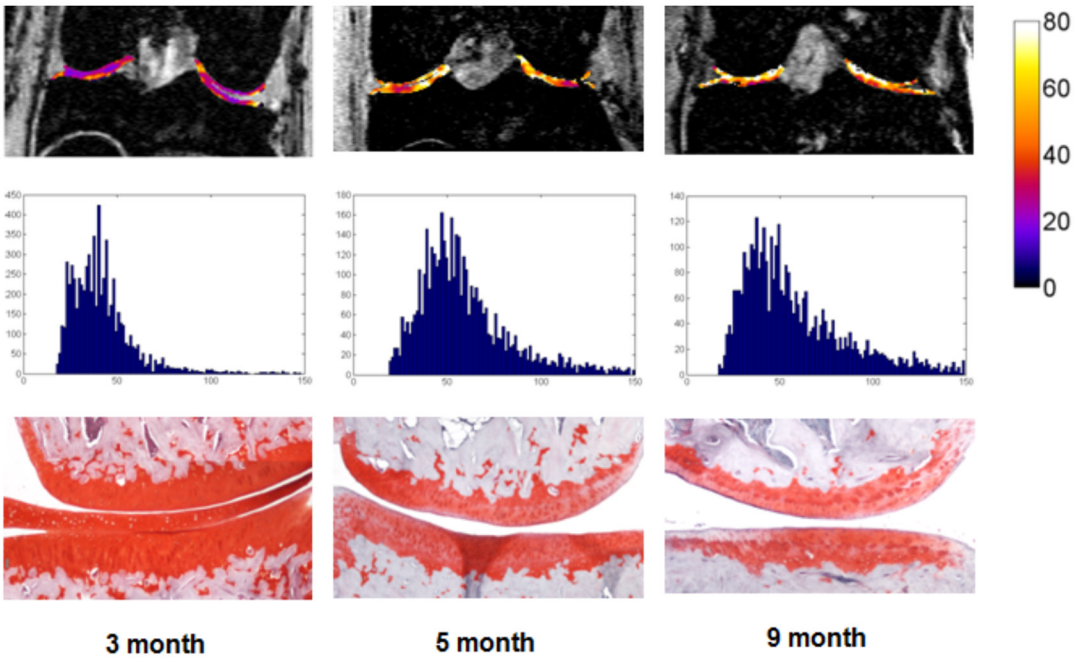

Figure 5.

Representative $T_{1\rho}$ maps in color (top row) are overlaid on $T_{1\rho}$ images from representative 3, 5, and 9 month old animals. Color bar on the right represents $T_{1\rho}$ value in milliseconds. Histograms of $T_{1\rho}$ values from these images and Safranin-O stained histology sections are shown below each image (middle and bottom rows, respectively). Both 5- and 9-month old animals displayed higher $T_{1\rho}$ values than the 3 month old, and age-related loss of PG loss was confirmed with subsequent histology images stained for PG content.

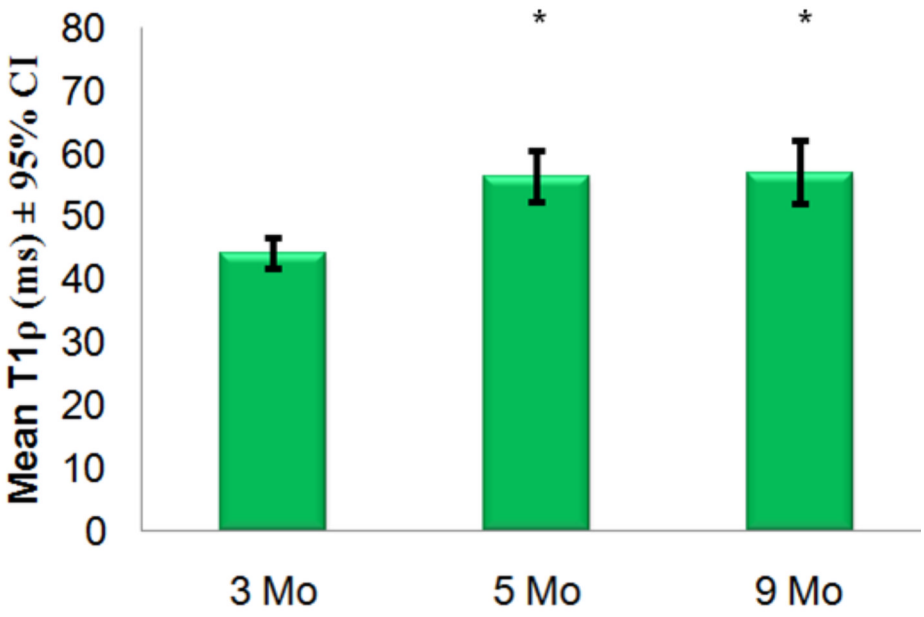

Figure 6.
Mean $T_{1\rho}$ values in each age cohort and 95% confidence intervals are plotted. Mean $T_{1\rho}$ was significantly different (*=$p<0.01$) between 3-month and both 5- and 9-month cohorts but not between 5- and 9-month cohorts.

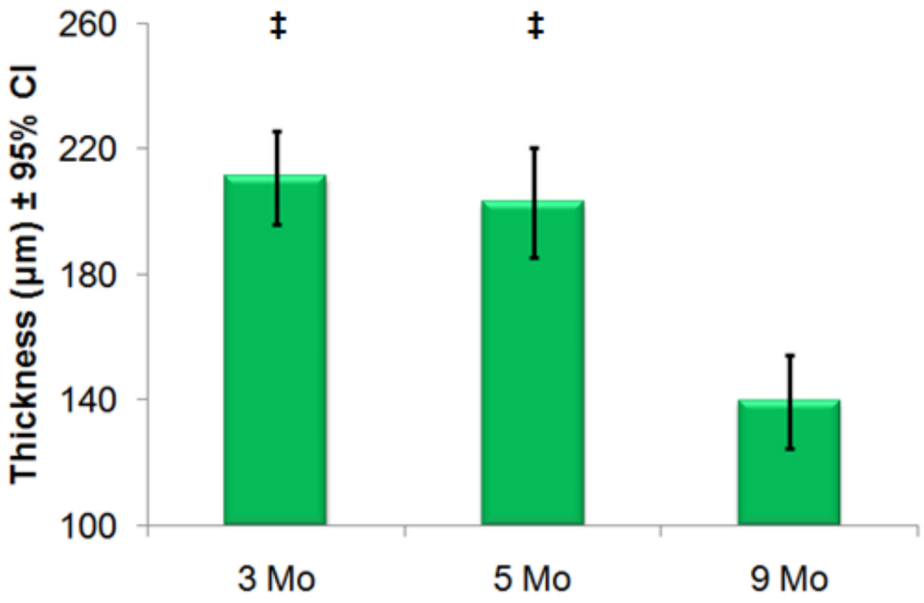

Figure 7.
Mean cartilage thickness measurements are plotted with 95% confidence intervals (CI). Values are recorded using high-resolution histology. There are significant differences (‡=$p<0.01$) between both the 3- and 5-month old animals compared to the 9-month cohorts but not between 3- and 5-month old cohorts.

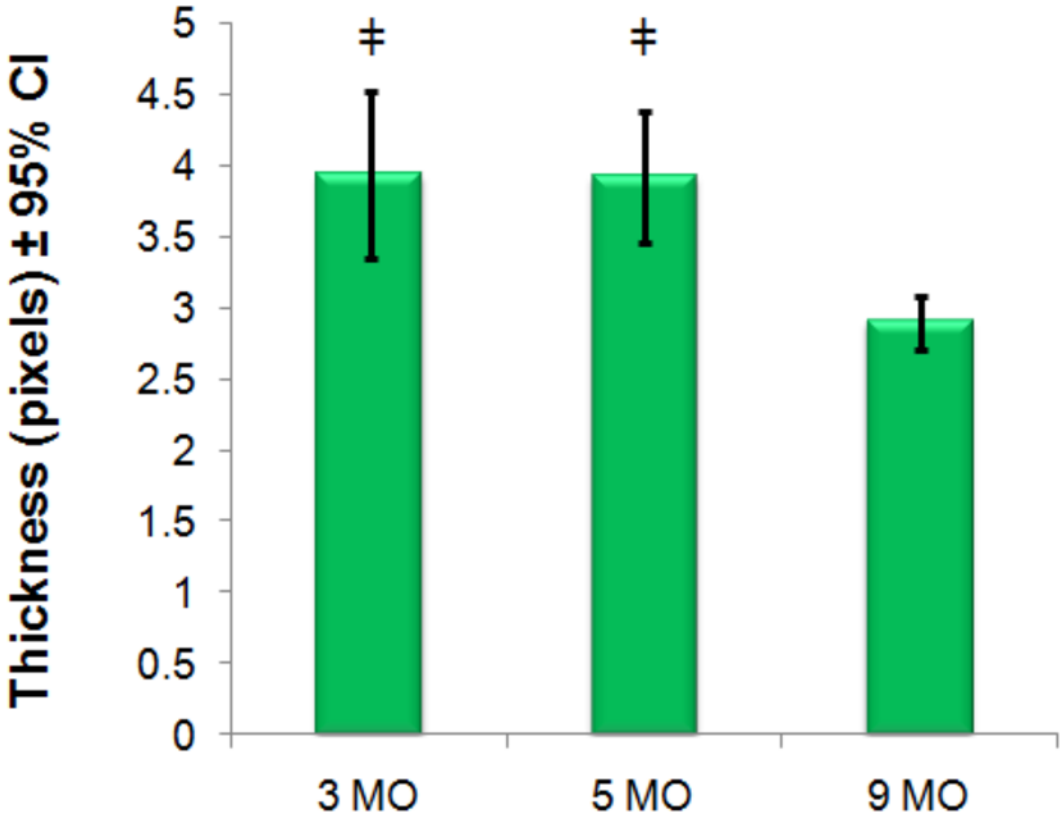

Figure 8.
Mean cartilage thickness measurements are plotted with 95% confidence intervals (CI). Values are recorded using T_1-weighted MRI. There are significant differences (‡=$p<0.01$) between both the 3- and 5-month old animals compared to the 9-month cohorts but not between 3- and 5-month old cohorts.

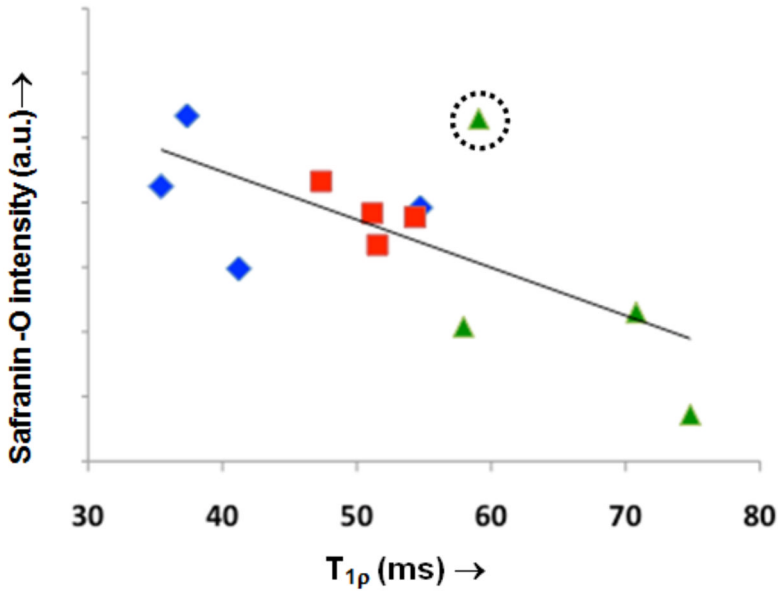

Figure 9.

Mean signal intensities from Safranin-O stained histology sections of each animal vs. their average $T_{1\rho}$. Where ◆ =3-month, ■ =5-month, and ▲ =9-month data. A moderate correlation (R^2=0.44, $p<0.01$) exists but is improved (R^2=0.67, $p<0.01$) if the outlier with abnormal and statistically significantly ($z=-2.2$) high stain intensity (indicated by dotted circle) is removed before analysis.

Table 1

Inter- and intra-animal Coefficients of Variation (CV) were determined from test-retest experiments for the $T_{1\rho}$ MRI protocol.

	Reproducibility		
	Animal 1	**Animal 2**	**Animal 3**
Mean Animal CV	6.51%	3.90%	9.29%
Mean Total CV	6.57%		